Author Manuscript

Author Manuscript

Author Manuscript

Author Manuscript

HHS Public Access

Author manuscript

Am J Surg Pathol. Author manuscript; available in PMC 2020 June 01.

Published in final edited form as:

Am J Surg Pathol. 2019 June ; 43(6): 851–860. doi:10.1097/PAS.0000000000001253.

Intratumoral Immune Response to Gastric Cancer Varies by Molecular and Histologic Subtype

Teresa S. Kim, M.D.[1], **Edaise da Silva, Ph.D.**[2], **Daniel G. Coit, M.D.**[3], **Laura H. Tang, M.D., Ph.D.**[2]

[1]Department of Surgery, University of Washington, Seattle, WA.

[2]Department of Pathology, Memorial Sloan Kettering Cancer Center, New York, NY.

[3]Department of Surgery, Memorial Sloan Kettering Cancer Center, New York, NY.

Abstract

Background: Immune checkpoint inhibition is effective in a subset of patients with advanced gastric cancer. Genomic profiling has revealed the heterogeneity of gastric adenocarcinomas, but the immune microenvironment and predictors of immunotherapy response remain poorly understood. We aimed to better characterize the underlying immune response to gastric cancer.

Methods: Retrospective review of a prospectively maintained institutional database was performed to identify patients who underwent curative intent resection of gastric adenocarcinoma from 2006–2016. Tumors were classified according to modified TCGA subtype: Epstein-Barr virus-associated (EBV), microsatellite instability-high (MSI), intestinal as a surrogate for chromosomal instability (CIN), diffuse as a surrogate for genomically stable (GS). Tumor infiltrating leukocytes (TIL) were measured using immunohistochemistry.

Results: Forty-three patients were identified: 6 EBV, 11 MSI, 14 intestinal, 12 diffuse. The most prevalent TIL were $CD8^+$ T lymphocytes and $CD68^+$ macrophages, comprising 15% and 13% of all tumor cells. EBV and MSI tumors were the most infiltrated, harboring 30–50% T cells and 20% macrophages. Intestinal tumors contained fewer T cells but disproportionately more macrophages. Diffuse tumors were the least infiltrated. Programmed cell death protein 1 (PD1) was most frequently expressed in intestinal tumors, whereas 70% of EBV and MSI tumors expressed programmed death-ligand 1 (PDL1).

Conclusion: We herein demonstrate a heterogeneous immune response to gastric cancer, which varies by tumor subtype and has implications for future immunotherapy trials. Checkpoint inhibition is unlikely to be effective as single-agent therapy against intestinal and diffuse tumors lacking prominent T cell infiltration or substantial PDL1 expression.

Corresponding author: Laura H. Tang MD, Ph.D., Memorial Sloan Kettering Cancer Center, 1275 York Avenue, New York, NY 10065, Tel: (212) 639-5905, Fax: (646) 422-2070, tangl@mskcc.org.

Conflicts of Interest

The authors have disclosed they have no significant relationships with, or financial interest in, any commercial companies pertaining to this article.

Author Manuscript Author Manuscript Author Manuscript Author Manuscript

Keywords

tumor microenvironment; programmed cell death protein 1 (PD1); programmed death-ligand 1 (PDL1); gastric cancer; microsatellite instability

INTRODUCTION

Despite advances in diagnostic imaging, surgical technique, and systemic therapy, gastric cancer remains the third leading cause of cancer-related death worldwide (1). Particularly among Western populations, patients tend to present with advanced-stage disease. Even for those patients with locoregional disease undergoing curative intent resection and perioperative chemotherapy, 5-year overall survival (OS) is less than 40% (2, 3), and median survival following recurrence is only 8 months (3). The need for more effective systemic therapies is evident.

Immunotherapy is being investigated in multiple solid tumors, including gastric cancer. Immune checkpoint inhibition, the most well-studied type, targets inhibitory receptors on T lymphocytes, such as cytotoxic T-lymphocyte associated protein 4 (CTLA4) and programmed cell death protein 1 (PD1), and releases effector T cells from negative feedback signaling. As has been observed in other tumors, such as melanoma and non-small cell lung cancer, a small subset of patients with advanced gastric cancer (10–20%) has been shown to respond to antibody-mediated blockade of CTLA4 (ipilimumab) and PD1 (nivolumab, pembrolizumab) (4–8). Among 493 heavily pretreated patients with advanced gastric cancer, the randomized phase III trial ONO-4538/ATTRACTION-2 demonstrated an objective response rate (ORR) of 11% and improved 12-month OS (26 versus 11%) among patients treated with nivolumab versus placebo (6). Earlier phase studies, including the phase Ib KEYNOTE-012 (7) and phase II KEYNOTE-059 (5) trials, demonstrated similar modest ORR to pembrolizumab (22% and 12%, respectively). Even among patients selected for tumor expression of programmed death-ligand 1 (PDL1), the cognate ligand for PD1, ORR remained low, 16–22% (5, 7). Two additional phase III trials of PD1/PDL1 inhibition did not demonstrate a survival benefit over standard cytotoxic chemotherapy (KEYNOTE-061, JAVELIN Gastric 300 Trial, reviewed by Cohen et al.) (4). Thus, although immune checkpoint inhibition represents a potential novel treatment strategy for advanced gastric cancer, more accurate predictors of response and improved understanding of resistance mechanisms are required.

Recent molecular profiling by The Cancer Genome Atlas (TCGA) has informed our understanding of the heterogeneous mechanisms underlying gastric cancer pathogenesis (9). Moving beyond Lauren classification of intestinal versus diffuse/signet-ring cell histologic subtypes (10), it is now evident that there are at least four molecular subtypes of gastric adenocarcinoma, including those associated with Epstein-Barr virus infection (EBV) with associated amplification of the genes encoding PDL1 and PDL2, those with microsatellite instability (MSI) often due to *MLH1* hypermethylation, those with frequent somatic copy number aberrations (chromosomal instability, CIN) enriched among intestinal type tumors, and those with genomic stability (GS) enriched among diffuse type tumors (9).

Author Manuscript Author Manuscript Author Manuscript Author Manuscript

A similar definition of the intrinsic immune landscape in gastric cancer is lacking, a definition that may be essential to predicting immunotherapy response and designing optimal treatment strategies. Preliminary studies have demonstrated increased inflammation and PDL1 expression in EBV- and MSI-associated gastric cancers (11–14). However, the frequency and function of specific tumor infiltrating leukocytes (TIL), and the relationship to tumor subtype, remain unknown. We hypothesized that there is a pre-existing immune response to gastric cancer, which varies by the pathobiology of tumor subtype. To test our hypothesis and better define the gastric cancer immune microenvironment, we characterized the intratumoral immune infiltrate in 43 human gastric adenocarcinomas, representing each of the four major biologic subtypes: EBV, MSI, Lauren intestinal tumors as a surrogate for CIN, and Lauren diffuse/signet-ring cell tumors as a surrogate for GS. We herein present tumor immunoprofiling results for each of the biologic subtypes of gastric cancer.

MATERIALS AND METHODS

Case Selection

Retrospective review of a prospectively maintained institutional database was performed to identify patients who underwent curative intent resection of histologically confirmed gastric adenocarcinoma between 2006 and 2016 at Memorial Sloan Kettering Cancer Center (MSKCC). Patients with gastroesophageal junction tumors were excluded. Patients who received preoperative chemotherapy or radiation, presented with metastatic disease, or endorsed a history of chronic immunosuppression were also excluded. Eligible patients with sufficient tissue archived for analysis were then identified for further histologic and molecular review as detailed below. Clinical and pathologic information was collected from patient charts. Pathologic tumor and nodal stage was assigned based on the eighth edition of the American Joint Committee on Cancer (AJCC) staging manual (15). Neutrophil and lymphocyte counts were obtained from peripheral blood complete blood count (CBC) analysis performed within three months prior to initial surgical resection. The study was approved by the MSKCC Institutional Review Board.

Histopathologic and Molecular Tumor Classification

Hematoxylin and eosin-stained (H&E) tissue sections and formalin-fixed paraffin-embedded (FFPE) blocks were retrieved from the Pathology archives at MSKCC. H&E slides from the entire resection specimen of each eligible case were reviewed by an expert gastrointestinal pathologist (LHT). Cases deemed to have adequate tissue, including a representative section containing both primary tumor and adjacent normal tissue, were then selected to provide broad representation of tumor and nodal stage as well as biologic subtype.

Adenocarcinomas were classified into one of four major subtypes based on molecular and histologic analysis (9, 10): (1) Epstein-Barr virus-associated (EBV), confirmed by in situ hybridization of EBV-encoded RNA (EBER); (2) microsatellite instability-high (MSI), assessed by IHC of DNA mismatch repair (MMR) proteins MLH1, PMS2, MSH2, and MSH6; (3) intestinal, as a surrogate for the TCGA chromosomal instability (CIN) type, arising from a background of chronic gastritis, intestinal metaplasia, atrophy, and a spectrum of glandular dysplasia; (4) diffuse/signet-ring cell, as a surrogate for the TCGA genomically

Author Manuscript Author Manuscript Author Manuscript Author Manuscript

stable (GS) type, with no evidence of gland-forming intestinal component or excessive extracellular mucin pools, and without apparent chronic gastritis, atrophy, intestinal metaplasia or precursor dysplasia. Because gastric specimens were not routinely tested for EBV infection or MSI status prior to 2014, eligible cases were screened for morphologic characteristics which were suggestive of EBV infection or MSI status, including medullary carcinoma with lymphoid stroma, increased tumor infiltrating lymphocytes, or intratumoral heterogeneity during H&E review, with subsequent molecular confirmation of EBV or MSI status as detailed above. The study cohort was enriched for the rarer EBV and MSI subtypes in order to achieve adequate numbers of patients per tumor subtype and hence statistical power to detect differences between each of the four subtypes.

For each selected case, the most representative section of tumor and adjacent normal tissue was identified for further immune profiling.

Tumor Immune Profiling

Tumor infiltrating leukocytes (TIL) were defined as follows: $CD4^+$ T lymphocytes (including helper and regulatory T cells), $CD8^+$ cytotoxic T lymphocytes, $FOXP3^+$ regulatory T lymphocytes (Treg), $CD20^+$ B lymphocytes, and $CD68^+$ macrophages. TIL were quantified and characterized by IHC using the following human-specific antibodies (clone, dilution): CD4 (SP35, 1:50), programed cell death protein 1 (PD1) (MRQ22, 1:500) from Cell Marque; CD8 (SP57, undiluted), CD163 (MRQ-26, undiluted) from Ventana; CD20 (L26, 1:2000), CD68 (KP1, 1:2000), major histocompatibility complex class II (MHC-II, HLA-DR) (TAL.1B5, 1:200), from DAKO; FOXP3 (236A/E7, 1:500) from AbCam; matrix metalloproteinase 9 (MMP9) (Ab3, 1:1000) from Oncogene Science; programmed death-ligand 1 (PDL1) (E1L3N, 1:500) from Cell Signaling.

Immunohistochemical labeling of CD4, CD8, CD20, CD68, CD163, HLA-DR, and PD1 was performed using Cell Conditioning 1 (mild) for antigen retrieval and the avidin-biotin-peroxidase detection system on the Ventana Discovery XT automated stainer (Ventana Medical Systems, Tucson, AZ). Immunohistochemical labeling of FOXP3, PDL1, and MMP9 was performed using Epitope Retrieval Solution 2 for antigen retrieval and the avidin-biotin-peroxidase detection system on the Leica automated stainer (Leica Biosystems, Nussloch, Germany). All cases were visualized using 3,3’-diaminobenzidine (DAB) as the chromogen.

Slides were digitized using the ScanScope XT scanner (Aperio Technologies, Vista, CA, USA). Scanned images were reviewed in ImageScope (Aperio Technologies), and five representative high-power fields (HPF, 0.25 mm^2) were selected per tumor section. Each HPF was saved in tagged image file format (TIFF). The TIFF images were then separated into hematoxylin and DAB channels using the Colour Deconvolution algorithm in FIJI/ImageJ software (National Institutes of Health, Bethesda, MD) (16, 17). The total number of cells were counted by segmenting the hematoxylin channel, and the count of cells positive for DAB signal was tabulated in a macro. Cell frequency was then calculated by dividing the number of DAB-positive cells by the total number of cells per HPF, and then calculating the mean cell frequency across five HPFs per tumor.

Author Manuscript Author Manuscript Author Manuscript Author Manuscript

Statistics

Mean intratumoral cell frequencies were compared using unpaired 2-tailed Student's *t* test or one-way ANOVA with Tukey's multiple comparisons test, as applicable. Categorial variables were compared using χ^2 test. Correlations were assessed with linear regression and Pearson correlation coefficient. All data were analyzed using GraphPad Prism 7 for Mac OS X, Version 7.0c (GraphPad Software, Inc., La Jolla, CA). A p-value < 0.05 was considered significant.

RESULTS

Clinicopathologic Features of the Study Cohort

Retrospective review of a prospectively maintained institutional database identified 982 patients who underwent curative intent gastrectomy for gastric adenocarcinoma during the study period 2006–2016. Six hundred one (61%) received no preoperative chemo- or radiotherapy. Among these treatment-naïve patients, 43 cases of resected gastric adenocarcinoma were identified with adequate tissue for immunoprofiling and broad representation of tumor and nodal stage as well as tumor subtype (Table 1). Cases were classified into four biologic subtypes based on Lauren histologic subtype (10), Epstein-Barr virus (EBV)-encoded RNA (EBER) in situ hybridization, and DNA mismatch repair (MMR) expression: EBV (N = 6), microsatellite instability-high (MSI, N = 11), intestinal as a surrogate for chromosomal instability (CIN, N = 14), and diffuse/signet-ring cell as a surrogate for genomically stable (GS, N = 12). The study cohort comprised of similar proportions of tumor subtypes as the TCGA cohort, with the exception of fewer intestinal/CIN cases (33 versus 50%) (9). By design, the study cohort was also enriched for EBV and MSI cases (14 and 26% respectively), in contrast to a recently published series of later-stage metastatic esophagogastric cancer patients from our institution (< 5% of each subtype) (18).

Clinical and pathologic features of the study cohort are further detailed in Table 1. Median age of the cohort was 68 years (range 20–92), with slight male predominance (56%). Pathologic tumor (T) and nodal (N) stages were distributed across each biologic tumor subtype, with a non-significant trend toward higher stage, i.e., more transmural disease and nodal spread, in the diffuse and intestinal groups.

$CD8^+$ T Cells and Macrophages Predominate the Gastric Cancer Immune Microenvironment

Comprehensive immunoprofiling revealed that $CD8^+$ cytotoxic T lymphocytes (CTL) and $CD68^+$ macrophages were the most prevalent tumor-infiltrating leukocytes (TIL) among the entire cohort, representing 15% and 13% of all intratumoral cells respectively (Fig. 1A–B). $CD4^+$ T cells were slightly less frequent (11%), with the $FOXP3^+$ regulatory T cell subset (Treg) representing only 3% of all cells (Fig. 1A–B). Intratumoral $CD8^+$ and $CD4^+$ T cell densities correlated with each other and with macrophage density (Fig. 1C). $CD20^+$ B cells minimally infiltrated tumors of any subtype (not shown).

Author Manuscript Author Manuscript Author Manuscript Author Manuscript

To determine whether the pattern of immune infiltration differed across tumor subtypes, TIL subsets were quantified within each group (Fig. 1D). Similar to the entire cohort, EBV tumors were most infiltrated with $CD8^+$ CTL and macrophages (28% and 22% of all intratumoral cells, respectively), with an intermediate frequency of $CD4^+$ T cells (20%) and low rate of Treg (4%). MSI and intestinal tumors each contained similar frequencies of CTL and macrophages (19% in MSI, 13–14% in intestinal). Conversely, diffuse tumors were most infiltrated by $CD8^+$ and $CD4^+$ T cells (7–8%) and contained disproportionately fewer macrophages (2%).

TIL were most commonly observed in a diffuse pattern throughout the tumor (Fig. 1A). A subset of MSI and intestinal tumors (8/11 and 5/14 cases, respectively) demonstrated an accumulation of macrophages, and to a lesser extent T cells, at the invasive front, i.e., deep margin of the tumor (Fig. 4D).

EBV and MSI are the Most Inflamed Gastric Cancer Subtypes

Among the four biologic subtypes of gastric cancer, EBV and MSI tumors had the largest immune infiltrate (Fig. 2). In fact, EBV tumors contained more TIL than actual tumor cells, comprised on average of 50% T cells and 20% macrophages (Fig. 2A, 2C). MSI tumors were slightly less inflamed, consisting on average of 30% T cells and 20% macrophages. Intestinal tumors were even less infiltrated, with about one-third of cells comprised of TIL, and diffuse tumors were the least inflamed, albeit still with nearly 20% TIL (Fig. 2A, 2C). Macrophages were disproportionately less frequent in diffuse tumors (Fig. 2C), but there were no significant differences in $CD8^+$ CTL/Treg ratio across tumor subtypes (Fig. 2B).

Generally, tumors with deeper mural invasion, i.e., higher T stage, were less infiltrated with T cell subsets and macrophages (Fig 2D, top). However, the opposite trend was observed in $CD8^+$ T cell infiltration in intestinal-type tumors, wherein transmural tumors harbored the most cytotoxic T cells (Fig. 2D, bottom). Among the study cohort, intestinal tumors also uniquely demonstrated a correlation between intratumoral Treg frequency and peripheral blood neutrophil-to-lymphocyte ratio (NLR), a marker of systemic inflammatory state (Fig. 2E and Supplemental Fig. S2). A similar but non-significant trend was observed in intestinal-type macrophage infiltration and NLR ($p = 0.3$, Fig. 2E and Supplemental Fig. S2). Overall, tumor subtype influenced the relationship between intratumoral immune infiltration and assorted clinicopathologic factors.

Programmed Cell Death Protein 1 (PD1)/Programmed Death-Ligand 1 (PDL1) Checkpoint Expression Varies by Tumor Subtype

To investigate potential immune evasion mechanisms across gastric cancer subtypes, we first assessed intratumoral expression of the clinically relevant T cell checkpoint receptor, programed cell death protein 1 (PD1), and one of its cognate ligands, programmed death-ligand 1 (PDL1). PD1 expression was observed in TIL of EBV, MSI, and intestinal tumors, comprising on average 6–10% of all intratumoral cells, with the highest frequency in intestinal tumors (Fig. 3A–B).

PDL1 ligand expression was also observed in non-diffuse tumor subtypes, with $PDL1^+$ TIL and tumor cells comprising 4–7% of all intratumoral cells (Fig. 3A, 3C). Diffuse tumors

Author Manuscript Author Manuscript Author Manuscript Author Manuscript

demonstrated minimal PD1 or PDL1 expression. Based on the minimum threshold of 1% of cells staining positive for PDL1 used in clinical trials of anti-PD1 immunotherapy (6, 7), 70% of EBV and MSI tumors in the cohort were PDL1-positive, whereas only 36% of intestinal and 17% of diffuse tumors were PDL1-positive. Hence, the PD1/PDL1 axis was most prominent in inflamed EBV and MSI tumors, and, to a lesser extent, in intestinal tumors.

Gastric Cancer-Associated Macrophages Exhibit Mixed M1- and M2-Like Phenotype

To further investigate potential mechanisms of tumor-mediated immunosuppression, particularly in those subtypes demonstrating low PD1/PDL1 expression, we sought to better characterize the intratumoral myeloid infiltrate. Across multiple solid tumor types, macrophages have been implicated in tumorigenesis, more often resembling the alternatively-activated, M2-like phenotype, with the ability to suppress anti-tumoral immunity and induce pro-tumoral effects such as angiogenesis and metastasis (19, 20).

Within our cohort of 43 gastric cancers, macrophages were one of the most frequently infiltrating immune cells in EBV, MSI, and intestinal tumors (Fig. 1). Phenotypic profiling demonstrated mixed expression of both immunosuppressive, M2-like markers, such as the scavenger receptor CD163 and matrix metalloproteinase 9 (MMP9) (Fig. 4A–B), and stimulatory M1-like markers, such as the major histocompatibility complex class II molecule (MHCII, HLA-DR) (Fig. 4C). Intestinal tumors exhibited a more M2-like or suppressive phenotype, with a non-significant trend in increased CD163 and MMP9 expression relative to HLA-DR (Fig. 4B–C). Intestinal tumors also demonstrated a non-significant association between intratumoral macrophage frequency and systemic NLR, unlike other tumor subtypes (Fig. 2E and Supplemental Fig. S2). Interestingly, diffuse tumors contained disproportionately more HLA-DR^{hi} cells (9%) compared with other TIL frequencies. These MHCII-expressing cells exhibited dendritic morphology on histology and could represent either M1-like macrophages or dendritic cells, another type of antigen-presenting cell.

From a spatial perspective, gastric cancer-associated macrophages most often infiltrated tumors diffusely (Fig. 1A, 4A, 4D, bottom). However, in over half of MSI tumors and one-third of intestinal tumors, CD68^{+} and CD163^{+} macrophages concentrated at the invasive front, i.e., the deep margin of the tumor (Fig. 4D, top). This pattern of infiltration was also seen to a lesser extent among T cells in MSI and intestinal tumors, but was only observed in 1/6 EBV and 0/12 diffuse tumors. Gastric cancer-associated macrophages thus represent a heterogeneous subset of TIL, with mixed M1- and M2-like phenotype, and variable infiltration based on tumor subtype.

DISCUSSION

The aim of the current study was to better define the underlying immune landscape in gastric adenocarcinoma. In a relatively large Western series of untreated tumors, i.e., surgical specimens from patients not receiving preoperative chemo/radiotherapy, we have observed that gastric cancer generates a heterogeneous immune response, one which parallels tumor-intrinsic molecular heterogeneity. Across the cohort of 43 patients, CD8^{+} cytotoxic T cells and CD68^{+} macrophages were the most common tumor infiltrating leukocytes (TIL).

Author Manuscript Author Manuscript Author Manuscript Author Manuscript

However, patterns of infiltration differed between biologic tumor subtypes. For example, EBV- and MSI-associated gastric cancers were the most inflamed, with more than half of all tumor cells consisting of immune cells. Intestinal tumors harbored fewer TIL than expected, given the association with chronic inflammation and *Helicobacter pylori* infection, but contained the highest density of $PD1^+$ cells and a disproportionate number of macrophages. Intestinal tumors also demonstrated a unique correlation between intratumoral Treg frequency and peripheral NLR, suggesting an association between local and systemic inflammation and defective antitumor immune response. Unlike other tumor subtypes, intestinal tumors also harbored more $CD8^+$ T cells in deeply invasive tumors, suggesting the presence but ineffectiveness of these intratumoral cytotoxic lymphocytes. Further translational studies will investigate the clonality and function of these specific gastric cancer TIL. By contrast, diffuse tumors were the least infiltrated but nevertheless comprised of more than 10% T cells.

Our results are comparable to prior studies, which primarily focused on EBV- and MSI-associated gastric cancers. An early report of 20 EBV-positive and 28 EBV-negative gastric cancers from van Beek et al. demonstrated larger immune infiltrate, higher frequency of activated granzyme B-expressing $CD8^+$ T cells, and more frequent CD8:CD4 T cell ratio > 1 in EBV-positive tumors (14). In a more recent series of 7 EBV, 16 MSI, and 21 non-EBV/MSI gastric cancers from Ma et al., EBV and MSI tumors demonstrated 2-fold higher density of $CD8^+$ T cells at the invasive front of the cancer, and a high rate of PDL1 positivity in up to 90–100% of cases (13). Similar rates of PDL1 positivity have been observed in other Western series (11, 12), as well as the current series, in which 70% of EBV and MSI tumors were PDL1-positive, whereas only 36% of intestinal and 17% of diffuse tumors were positive. Interestingly, while Ma et al. did not detect an independent association between immune infiltration and either tumor stage or survival, several other series have demonstrated conflicting results, with either a positive (21, 22) or negative (23, 24) association of PDL1 expression with survival. The true impact of immune profile on treatment response and clinical outcome remains to be determined. As immune checkpoint inhibition becomes increasingly studied in the clinical setting, our results highlight the importance of stratifying gastric cancer patients by biologic tumor subtype in future trials. While EBV and MSI tumors would be predicted to respond to immune checkpoint inhibition, single-agent PD1 or PDL1 blockade is unlikely to be effective against intestinal- or diffuse-type tumors, which harbor fewer $CD8^+$ cytotoxic T cells and lower PDL1 expression.

Macrophages represented the other major type of immune cell infiltrating non-diffuse subtypes of gastric cancer in our series. Phenotypic profiling of cell surface markers revealed mixed expression of stimulatory M1-like markers (MHC class II/HLA-DR) and inhibitory M2-like markers (CD163 scavenger receptor, matrix metalloproteinase MMP9), with a trend toward increased inhibitory marker expression in intestinal-type tumors. Limited studies of gastric cancer-associated macrophages in the literature report similar phenotypic heterogeneity (25), and variable association with survival (25, 26). One functional report of macrophages isolated from freshly resected human gastric cancers identified an inhibitory effect on tumor-infiltrating natural killer (NK) cells, mediated by the cytokine TGF-beta (27). In the current study, intestinal intratumoral macrophage infiltration demonstrated a

Author Manuscript Author Manuscript Author Manuscript Author Manuscript

non-significant correlation with peripheral blood NLR, a marker of systemic inflammation that has previously been shown to be an independent predictor of poor disease-specific survival among resectable gastric cancer patients treated with surgical resection and neoadjuvant chemotherapy (28). Interestingly, one of the 43 patients in the current series, with an MSI-high tumor, developed peritoneal recurrence after surgery, underwent treatment with anti-PD1 therapy for a year, and experienced a complete clinical response. Immune profiling of the primary tumor from this patient, compared with the remainder of the cohort, demonstrated the lowest density of macrophages, relatively high $CD8^+$ CTL/Treg ratio, and high PD1 but negligible PDL1 expression (Supplemental Fig. S1). Further investigation of macrophage function and polarization is warranted to identify potential biomarkers of response, resistance mechanisms, and new immunotherapeutic targets.

Notably, diffuse-type tumors in our series demonstrated an immune-desert phenotype (29), with minimal infiltration of immune cells, and particularly low density of macrophages. Few published reports specifically address the immune response to diffuse-type gastric cancers (30). The relatively high frequency of cells expressing the antigen-presenting MHC class II molecule (HLA-DR) is hence of particular interest, and will require validation in additional cohorts of diffuse gastric cancers, as well as further characterization of the relevant cell type, e.g., dendritic cell versus M1-like macrophage, or other stromal or tumor cell. Enhancing antigen presentation represents a promising strategy to increase immune recognition and activity against so-called immune-desert tumors (29).

Our study is limited by the retrospective design and descriptive nature, as well as the small case numbers within each tumor subtype, precluding multivariate analysis of immunologic variables and clinical outcomes. Nevertheless, sample size is comparable to other published Western series of gastric cancer immunity, and our study is unique in the exclusion of cases treated with preoperative chemotherapy or radiotherapy. We were therefore able to study the pre-existing immune response to gastric cancer without potential confounding effects of chemotherapy or radiation. This is pertinent in the context of preclinical studies demonstrating the immunologic effects of both platinum-based chemotherapy (31, 32) and radiation (33). Classification of tumors was also dependent on both molecular and histologic assessments, rather than the purely genomic classification defined by the TCGA (9). Considering the well-known intratumoral heterogeneity in gastric adenocarcinoma, random tumor tissue submitted for genomic analysis may not fully represent the underlying mechanisms of disease. Although our results for intestinal and diffuse tumors may thus differ from the immune profile of CIN and GS tumors, we believe the combined molecular and histologic classification utilized in the current study better defines the pathogenetic mechanisms of gastric cancer.

In sum, we herein present an overview of the heterogeneous immune landscape of gastric cancer, delving beyond PDL1 expression to quantify and characterize the major lymphoid and myeloid components and identify immune infiltration patterns according to biologic tumor subtype. Results have important implications on the development of future immunotherapy trials, i.e., immune checkpoint inhibition trials should be stratified not only by PDL1 expression, but also by histologic and molecular tumor subtype as a surrogate for $CD8^+$ T cell infiltration. Our findings also highlight key areas for future translational

Author Manuscript Author Manuscript Author Manuscript Author Manuscript

research, including targeting of inhibitory gastric cancer-associated macrophages, and development of rational combination strategies to enhance immune recognition of minimally inflamed diffuse-type tumors.

Supplementary Material

Refer to Web version on PubMed Central for supplementary material.

ACKNOWLEDGMENTS

We thank members of the Sloan-Kettering Institute Molecular Cytology Core Facility and Memorial Hospital Pathology Core Facility for assistance with immunohistochemistry and image analysis. We thank Drs. Yelena Janjigian, Ronald DeMatteo, and Murray Brennan for helpful discussions, and Ms. Tanisha Daniel for administrative support.

Source of Funding: Supported by the Mushett Family Foundation (LHT), the Peter and Linda Bren Fund for GI Cancer Research (DGC), and MSKCC Support Grant/Core Grant (P30 CA008748).

REFERENCES

1. Ferlay J, Soerjomataram I, Dikshit R, et al. Cancer incidence and mortality worldwide: sources, methods and major patterns in GLOBOCAN 2012. International journal of cancer Journal international du cancer. 2015;136:E359–386. [PubMed: 25220842]
2. Cunningham D, Allum WH, Stenning SP, et al. Perioperative chemotherapy versus surgery alone for resectable gastroesophageal cancer. N Engl J Med 2006;355:11–20. [PubMed: 16822992]
3. Lee JH, Chang KK, Yoon C, et al. Lauren Histologic Type Is the Most Important Factor Associated With Pattern of Recurrence Following Resection of Gastric Adenocarcinoma. Ann Surg 2018;267:105–113. [PubMed: 27759618]
4. Cohen NA, Strong VE, Janjigian YY. Checkpoint blockade in esophagogastric cancer. J Surg Oncol 2018.
5. Fuchs CS, Doi T, Jang RW, et al. Safety and Efficacy of Pembrolizumab Monotherapy in Patients With Previously Treated Advanced Gastric and Gastroesophageal Junction Cancer: Phase 2 Clinical KEYNOTE-059 Trial. JAMA Oncol 2018;4:e180013. [PubMed: 29543932]
6. Kang YK, Boku N, Satoh T, et al. Nivolumab in patients with advanced gastric or gastro-oesophageal junction cancer refractory to, or intolerant of, at least two previous chemotherapy regimens (ONO-4538–12, ATTRACTION-2): a randomised, double-blind, placebo-controlled, phase 3 trial. Lancet 2017;390:2461–2471. [PubMed: 28993052]
7. Muro K, Chung HC, Shankaran V, et al. Pembrolizumab for patients with PD-L1-positive advanced gastric cancer (KEYNOTE-012): a multicentre, open-label, phase 1b trial. The lancet oncology 2016;17:717–726. [PubMed: 27157491]
8. Janjigian YY, Bendell J, Calvo E, et al. CheckMate-032 Study: Efficacy and Safety of Nivolumab and Nivolumab Plus Ipilimumab in Patients With Metastatic Esophagogastric Cancer. J Clin Oncol 2018:JCO2017766212.
9. Cancer Genome Atlas Research N. Comprehensive molecular characterization of gastric adenocarcinoma. Nature. 2014;513:202–209. [PubMed: 25079317]
10. Lauren P The Two Histological Main Types of Gastric Carcinoma: Diffuse and So-Called Intestinal-Type Carcinoma. An Attempt at a Histo-Clinical Classification. Acta Pathol Microbiol Scand 1965;64:31–49. [PubMed: 14320675]
11. Derks S, Liao X, Chiaravalli AM, et al. Abundant PD-L1 expression in Epstein-Barr Virus-infected gastric cancers. Oncotarget 2016;7:32925–32932. [PubMed: 27147580]
12. Hissong E, Ramrattan G, Zhang P, et al. Gastric Carcinomas With Lymphoid Stroma: An Evaluation of the Histopathologic and Molecular Features. Am J Surg Pathol 2018;42:453–462. [PubMed: 29438172]

Author Manuscript Author Manuscript Author Manuscript Author Manuscript

13. Ma C, Patel K, Singhi AD, et al. Programmed Death-Ligand 1 Expression Is Common in Gastric Cancer Associated With Epstein-Barr Virus or Microsatellite Instability. Am J Surg Pathol 2016;40:1496–1506. [PubMed: 27465786]
14. van Beek J, zur Hausen A, Snel SN, et al. Morphological evidence of an activated cytotoxic T-cell infiltrate in EBV-positive gastric carcinoma preventing lymph node metastases. Am J Surg Pathol 2006;30:59–65. [PubMed: 16330943]
15. Amin MB, Edge SB, American Joint Committee on Cancer AJCC cancer staging manual Switzerland: Springer; 2017.
16. Schindelin J, Arganda-Carreras I, Frise E, et al. Fiji: an open-source platform for biological-image analysis. Nat Methods 2012;9:676–682. [PubMed: 22743772]
17. Schneider CA, Rasband WS, Eliceiri KW. NIH Image to ImageJ: 25 years of image analysis. Nat Methods 2012;9:671–675. [PubMed: 22930834]
18. Janjigian YY, Sanchez-Vega F, Jonsson P, et al. Genetic Predictors of Response to Systemic Therapy in Esophagogastric Cancer. Cancer discovery. 2018;8:49–58. [PubMed: 29122777]
19. Mantovani A, Marchesi F, Malesci A, et al. Tumour-associated macrophages as treatment targets in oncology. Nat Rev Clin Oncol 2017;14:399–416. [PubMed: 28117416]
20. Qian BZ, Pollard JW. Macrophage diversity enhances tumor progression and metastasis. Cell 2010;141:39–51. [PubMed: 20371344]
21. Boger C, Behrens HM, Mathiak M, et al. PD-L1 is an independent prognostic predictor in gastric cancer of Western patients. Oncotarget 2016;7:24269–24283. [PubMed: 27009855]
22. Xing X, Guo J, Wen X, et al. Analysis of PD1, PDL1, PDL2 expression and T cells infiltration in 1014 gastric cancer patients. Oncoimmunology. 2018;7:e1356144. [PubMed: 29399387]
23. Thompson ED, Zahurak M, Murphy A, et al. Patterns of PD-L1 expression and CD8 T cell infiltration in gastric adenocarcinomas and associated immune stroma. Gut 2017;66:794–801. [PubMed: 26801886]
24. Schlosser HA, Drebber U, Kloth M, et al. Immune checkpoints programmed death 1 ligand 1 and cytotoxic T lymphocyte associated molecule 4 in gastric adenocarcinoma. Oncoimmunology. 2016;5:e1100789. [PubMed: 27467911]
25. Zhang H, Wang X, Shen Z, et al. Infiltration of diametrically polarized macrophages predicts overall survival of patients with gastric cancer after surgical resection. Gastric Cancer. 2015;18:740–750. [PubMed: 25231913]
26. Huang X, Pan Y, Ma J, et al. Prognostic significance of the infiltration of CD163(+) macrophages combined with CD66b(+) neutrophils in gastric cancer. Cancer Med 2018;7:1731–1741. [PubMed: 29573574]
27. Peng LS, Zhang JY, Teng YS, et al. Tumor-Associated Monocytes/Macrophages Impair NK-Cell Function via TGFbeta1 in Human Gastric Cancer. Cancer Immunol Res 2017;5:248–256. [PubMed: 28148545]
28. Wang SC, Chou JF, Strong VE, et al. Pretreatment Neutrophil to Lymphocyte Ratio Independently Predicts Disease-specific Survival in Resectable Gastroesophageal Junction and Gastric Adenocarcinoma. Ann Surg 2016;263:292–297. [PubMed: 25915915]
29. Chen DS, Mellman I. Elements of cancer immunity and the cancer-immune set point. Nature 2017;541:321–330. [PubMed: 28102259]
30. Kim JW, Nam KH, Ahn SH, et al. Prognostic implications of immunosuppressive protein expression in tumors as well as immune cell infiltration within the tumor microenvironment in gastric cancer. Gastric Cancer. 2016;19:42–52. [PubMed: 25424150]
31. Pfirschke C, Engblom C, Rickelt S, et al. Immunogenic Chemotherapy Sensitizes Tumors to Checkpoint Blockade Therapy. Immunity 2016;44:343–354. [PubMed: 26872698]
32. Galluzzi L, Buque A, Kepp O, et al. Immunogenic cell death in cancer and infectious disease. Nat Rev Immunol 2017;17:97–111. [PubMed: 27748397]
33. Weichselbaum RR, Liang H, Deng L, et al. Radiotherapy and immunotherapy: a beneficial liaison? Nat Rev Clin Oncol 2017;14:365–379. [PubMed: 28094262]

Author Manuscript Author Manuscript Author Manuscript Author Manuscript

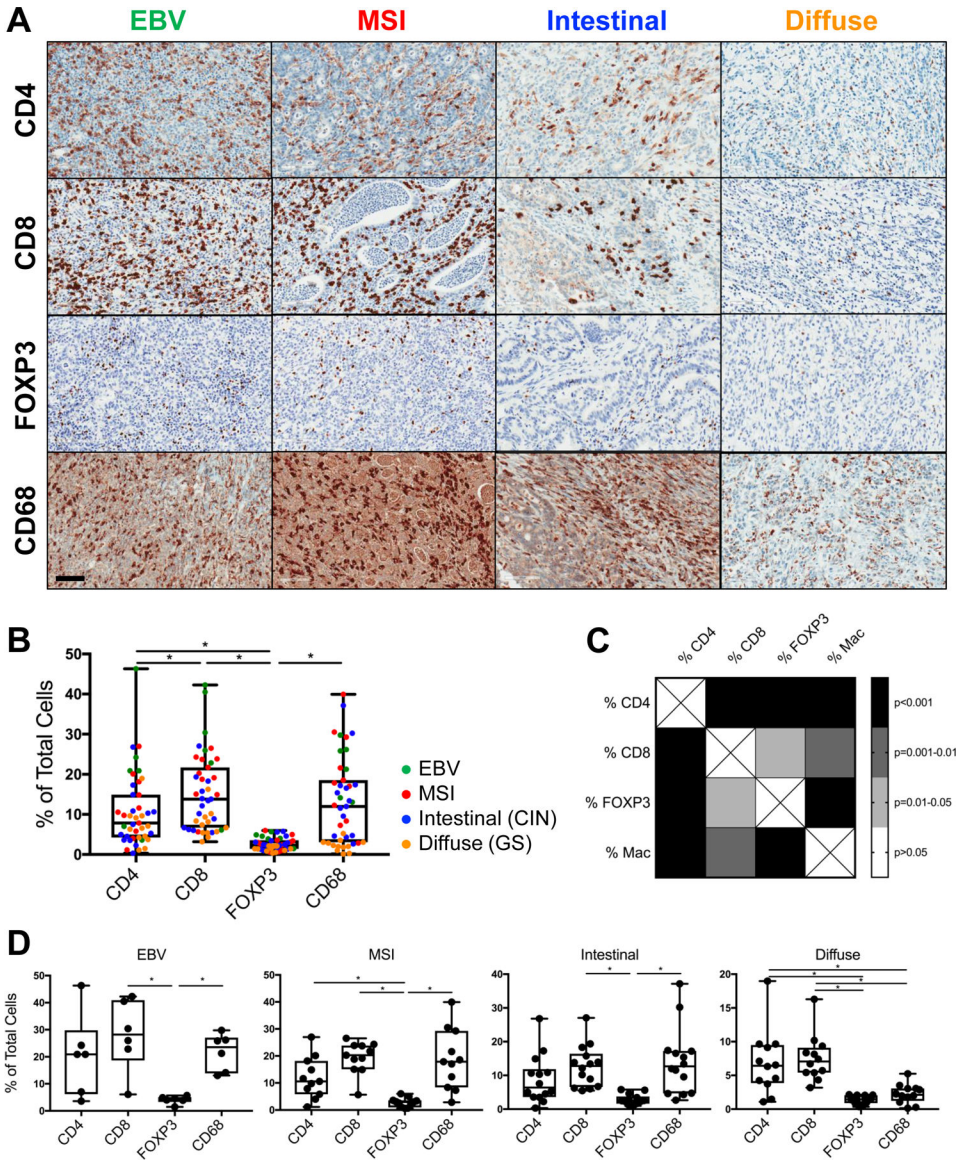

Figure 1.

$CD8^+$ T cells and $CD68^+$ macrophages are the most prevalent immune cells infiltrating human gastric cancer. A, Representative immunohistochemistry (IHC) of the most common tumor-infiltrating leukocytes (TIL), including $CD4^+$ and $CD8^+$ T cells, $FOXP3^+$ regulatory T cells (Treg), and $CD68^+$ macrophages, in EBV, MSI, intestinal, and diffuse subtypes of gastric cancer. Scale bar: 100 μm. B, Quantification of TIL frequencies as a percentage of all intratumoral cells, as measured by IHC. C, Correlation matrix demonstrating associations between the major TIL subsets quantified in B. D, Quantification of TIL frequencies for each of the 4 biologic subtypes of gastric cancer. Each data point represents a unique patient's tumor (N = 43, including 6 EBV, 11 MSI, 14 intestinal, and 12 diffuse gastric cancers). Box plots represent the median and all data points within the min-max range. *, $P < 0.05$.

Author Manuscript Author Manuscript Author Manuscript Author Manuscript

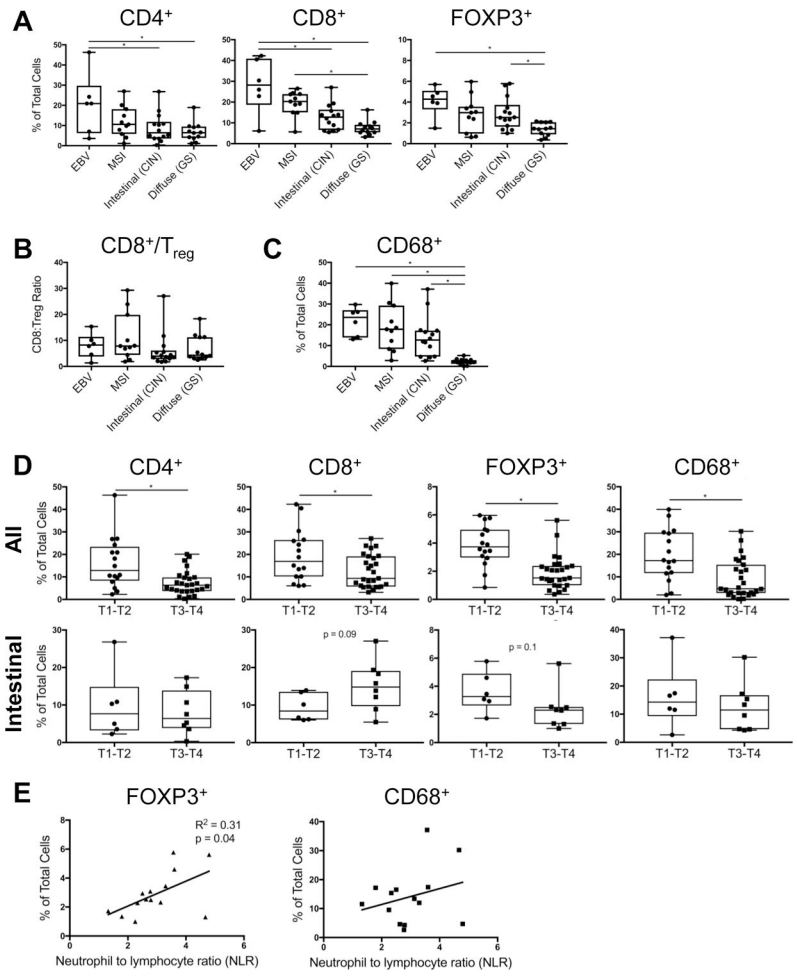

Figure 2.

EBV and MSI are the most inflamed subtypes of gastric cancer. A, Intratumoral T cell frequencies were compared across the 4 gastric cancer subtypes, based on CD4, CD8, and FOXP3 IHC demonstrated in Figure 1. B, $CD8^+$ cytotoxic T cell/$FOXP3^+$ Treg ratio was calculated for each tumor subtype. C, Intratumoral macrophage frequency was compared across tumor subtypes, based on CD68 IHC. D, Intratumoral immune cell frequencies in tumors with low versus high tumor (T) stage (T1–2 versus T3–4), within the entire study cohort (top) and intestinal/CIN subtype (bottom). E, Association between intratumoral $FOXP3^+$ Treg or $CD68^+$ macrophage frequency and peripheral blood neutrophil-to-lymphocyte (NLR) ratio, within intestinal/CIN tumors. Each data point represents a unique patient's tumor (N = 43, including 6 EBV, 11 MSI, 14 intestinal, and 12 diffuse gastric cancers). Box plots represent the median and all data points within the min-max range. *, $P < 0.05$.

Author Manuscript Author Manuscript Author Manuscript Author Manuscript

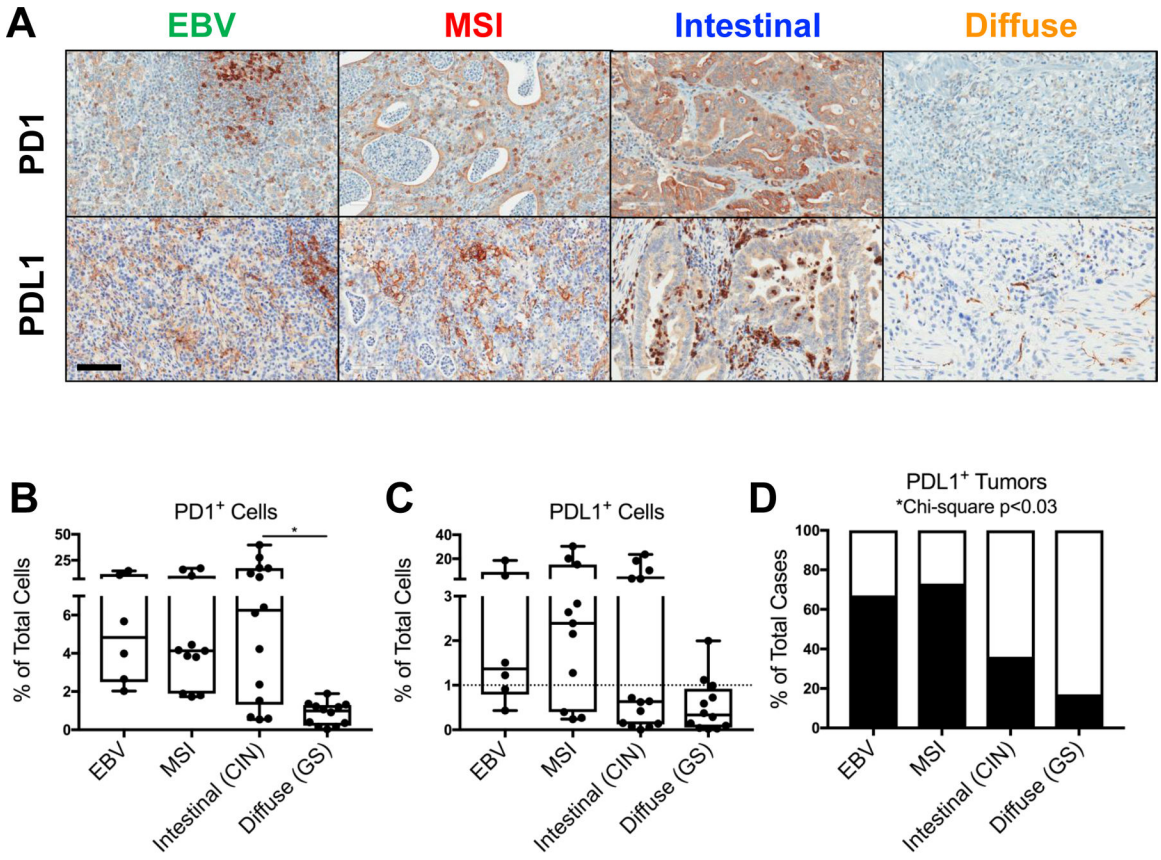

Figure 3.

Programmed cell death protein 1 (PD1)/programmed death-ligand 1 (PDL1) expression is highest in EBV and MSI tumors. A, Representative PD1 (top) and PDL1 (bottom) IHC within EBV, MSI, intestinal, and diffuse gastric cancers. Scale bar: 100 μm. B, Quantification of $PD1^+$ TIL within each tumor subtype, as measured by IHC. C-D, Quantification of $PDL1^+$ intratumoral cells, and the percentage of all cases defined as PDL1-positive (black bars), based on ≥ 1% of intratumoral cells staining positive for PDL1. Each data point represents a unique patient's tumor (N = 43, including 6 EBV, 11 MSI, 14 intestinal, and 12 diffuse gastric cancers). Box plots represent the median and all data points within the min-max range. *, $P < 0.05$.

Author Manuscript Author Manuscript Author Manuscript Author Manuscript

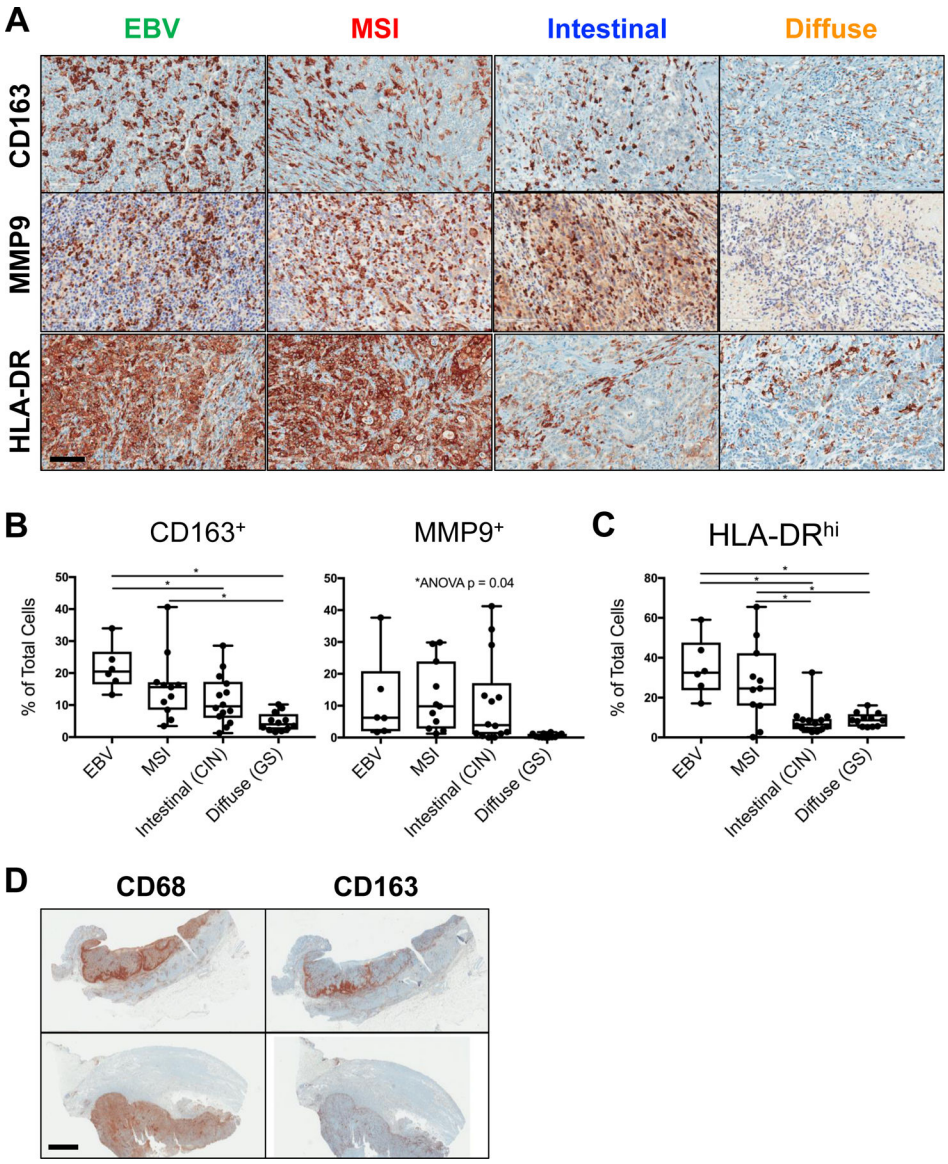

Figure 4.

Gastric cancer-associated macrophages are prevalent and exhibit mixed M1- and M2-like phenotype. A, Representative IHC of macrophage markers including CD163, matrix metalloproteinase 9 (MMP), and the major histocompatibility complex class II molecule (MHCII, HLA-DR), within EBV, MSI, intestinal, and diffuse gastric cancers. Scale bar: 100 μm. B-C, Quantification of $CD163^{+}$, $MMP9^{+}$, and $HLA\text{-}DR^{hi}$ TIL, as measured by IHC. D, Representative IHC demonstrating macrophage infiltration at the invasive front (top) versus diffusely throughout the tumor (bottom) in 2 different MSI gastric cancers. Scale bar: 4 mm. Each data point represents a unique patient's tumor (N = 43, including 6 EBV, 11 MSI, 14 intestinal, and 12 diffuse gastric cancers). Box plots represent the median and all data points within the min-max range. *, $P < 0.05$.

Author Manuscript Author Manuscript Author Manuscript Author Manuscript

Table 1.

Clinicopathologic characteristics by tumor subtype.

Characteristic	Total (43)		EBV (6)		MSI (11)		Intestinal (14)		Diffuse (12)		*P*
	N	%	N	%	N	%	N	%	N	%	
Age, median (range)	68 (20–92)		72 (40–85)		74 (55–85)		78 (52–92)		48 (20–67)		<0.01
Sex											0.02
Male	24	55.8	5	83.3	5	45.5	11	78.6	3	25.0	
Female	19	44.2	1	16.7	6	54.5	3	21.4	9	75.0	
Tumor location											<0.01
Upper	2	4.7	1	16.7	0	0	0	0	1	8.3	
Middle	14	32.6	4	66.7	5	45.5	0	0	5	41.7	
Lower	25	58.1	1	16.7	6	54.5	14	100	4	33.3	
Entire	2	4.7	0	0	0	0	0	0	2	16.7	
H. pylori infection											0.03
Absent	32	74.4	2	33.3	7	63.6	12	85.7	11	91.7	
Present	11	25.6	4	66.7	4	36.4	2	14.3	1	8.3	
NLR, mean (range)	3.0 (1.1–6.8)		3.8 (2.0–5.6)		3.1 (1.2–6.8)		3.0 (1.3–4.8)		2.5 (1.1–4.1)		0.19
Tumor stage											0.39
T1	9	20.9	3	50.0	3	27.3	3	21.4	0	0	
T2	7	16.3	1	16.7	2	18.2	3	21.4	1	8.3	
T3	15	34.9	2	33.3	3	27.3	4	28.6	6	50.0	
T4	12	27.9	0	0	3	27.3	4	28.6	5	41.7	
Lymphovascular invasion											0.07
Absent	13	30.2	4	66.7	2	18.2	2	14.3	5	41.7	
Present	30	69.8	2	33.3	9	81.8	12	85.7	7	58.3	
Perineural invasion											0.01
Absent	17	39.5	3	50.0	7	63.6	7	50.0	0	0	
Present	26	60.5	3	50.0	4	36.4	7	50.0	12	100.0	
Nodal stage											0.45
N0	18	41.9	4	66.7	5	45.5	5	35.7	4	33.3	
N1	6	14.0	1	16.7	2	18.2	3	21.4	0	0	
N2	10	23.3	0	0	3	27.3	4	28.6	3	25.0	
N3	9	20.9	1	16.7	1	9.1	2	14.3	5	41.7	

EBV, Epstein-Barr virus-associated; MSI, microsatellite instability-high; NLR, neutrophil to lymphocyte ratio at diagnosis